Desalination and Water Treatment
www.deswater.com
doi: 10.1080/19443994.2015.1119737

57 (2016) 21091–21104
September

Taylor & Francis
Taylor & Francis Group

Microwave-induced H_2SO_4 activation of activated carbon derived from rice agricultural wastes for sorption of methylene blue from aqueous solution

Somaye Mashhadi[a], Hamedreza Javadian[a,*], Maryam Ghasemi[a], Tawfik A. Saleh[b], Vinod Kumar Gupta[b,c,d]

[a]*Young Researchers and Elite Club, Arak Branch, Islamic Azad University, Arak, Iran, email: somayemashhadi@gmail.com (S. Mashhadi), Tel. +98 911 2160238; emails: hamedreza.javadian@yahoo.com (H. Javadian), m.gh6282@gmail.com (M. Ghasemi)*
[b]*Department of Chemistry, King Fahd University of Petroleum & Minerals, Dhahran, Saudi Arabia, emails: tawfik@kfupm.edu.sa (T.A. Saleh), vinodfcy@gmail.com (V.K. Gupta)*
[c]*Department of Chemistry, Indian Institute of Technology Roorkee, Roorkee 247667, India*
[d]*Department of Applied Chemistry, University of Johannesburg, Johannesburg, South Africa*

Received 17 February 2015; Accepted 16 October 2015

ABSTRACT

Activated carbon derived from the rice straw was used for the rapid removal and fast adsorption of methylene blue (MB) from the solvent phase of the aqueous solution. The developed adsorbent was characterized using various analytical techniques such as scanning electron microscopy and FTIR. The effect of various influential parameters including solution pH, adsorbent dosage, contact time, initial adsorbate concentration, stirring speed, and temperature on MB removal were well investigated and optimized. The experimental optimized data showed that a maximum amount of MB ions can be removed at contact time 25 min, dye ion concentration 40 mg/L, and pH of 7. The obtained results of the isotherm study revealed that adsorption data was in good agreement with Langmuir isotherm model (with R^2 value of 0.988 and maximum adsorption capacity of 62.5 mg/g at initial pH of 7 and temperature of 298 K). The negative values of ΔG° and the positive values of ΔH° (22.73 kJ/mol) and ΔS° (104 J/mol K) showed that the adsorption process was a spontaneous physical adsorption process i.e. endothermic and entropy driven.

Keywords: Active carbon; Cationic dye; Agricultural waste; Methylene blue; Removal

1. Introduction

Dyes and pigments are used in various industries such as paper, textiles, leather, plastics, rubber, cosmetics, and food beverages [1]. Colored and textile industries wastewaters are one of major sources that lead to the environmental contamination [2]. Methylene blue (MB) (3,7-bis (Dimethylamino)-phenothiazin-5-iumchloride) known as cationic dye is an important class of aromatic chemicals that are used in the coloring and textile industries. MB is also used for coloring paper, as temporary hair colorant, dyeing cottons and wools. However, it is not highly dangerous, but it possesses some adverse effects such as increase in hypertension, nausea, diarrhea, headache, dizziness,

*Corresponding author.

and eye injuries and opthial irritation in *Homo sapiens*. Thus, it is needed to be removed before the sewage disposal into the aqueous streams [3–5]. Several physical and chemical processes are used such as photo-decomposition and ultrafiltration, coagulation and flocculation, membrane filtration, electrochemical techniques, precipitation, ozonation, biosorption, and adsorption [6,7]. Among all the adsorption is a best physicochemical method which is an efficient and economic technique for removing the noxious dyes, pigments, and other colorants [8,9]. Among adsorbents, adsorption onto activated carbon is an effective and reliable method. Activated carbons have the advantages of exhibiting a high adsorption capacity for dyes due to their large surface area, microporous structure, adequate pore size distribution and porosity, high degree of surface reactivity and relatively high mechanical strength [10–12]. Activated carbon prepared from agricultural wastes helps to solve their disposal problem and also can be used as an efficient low-cost adsorbent. Agricultural wastes include orange peel, rice husk and straw, jute fiber, soy meal hull, coconut shells, corn cobs, Cotton stalks, wheat shells, activated date pit, and bamboo dust [13,14]. Many of the activated carbons were produced by a two-step process carbonization followed by activation. The carbonization is to enrich the carbon content and to create an initial porosity. The activation process helps in enhancing the pore structure. The activations are obtained by two procedures: physical activation or chemical activation [15,16]. In physical activation, the precursor is placed at high temperatures (ranging of 800–1,100˚C) in the presence of oxidizing agents such as air, water steam, CO_2, or a mixture of them [17–19]. In chemical activation, the precursor is mixed with a concentrated solution of an activating agent, e.g. phosphoric acid, zinc chloride, sulfuric acid, and potassium iodide, which causes the formation of porous structures in the material. Chemical activation is done at temperatures less than physical activation temperatures (ranging of 400–600˚C), allowing the achievement of activated carbons with higher efficiency due to dehydrogenation capability of the activating agent, which inhibits the production of volatile matters during the activation process [20,21]. On the basis of our researches, limited investigations on the preparation of activated carbons from rice straw using sulfuric acid as activating agent are carried out; there are relatively limited studies in the preparation of rice straw by microwave radiation [22–24]. Moreover, preparation of activated carbon using microwave radiation has attracted considerable attention as a green technology.

In the present work, the ability of low-cost adsorbents such as agricultural wastes (Rice straw) for the rapid removal and fast adsorption of MB from aqueous solution was well investigated and elucidated. Various influential parameters including solution pH, adsorbent dose, contact time, initial adsorbate concentration, stirring speed, and temperature on color removal were well studied and optimized. Moreover, MB adsorption isotherm, mechanisms with kinetic and thermodynamic models were measured and discussed.

2. Experimental

2.1. Reagents and instruments

All chemicals used were of analytical reagent grade. Potassium hydroxide (KOH), sodium hydroxide (NaOH), and sulfuric acid (H_2SO_4) were purchased from Sigma-Aldrich, USA. Methylene blue (MB, 3,7-bis(Dimethylamino)-phenothiazin-5-iumchloride) was purchased from DyStar Co. (Germany). All the reagents used were of analytical grade and doubly distilled deionized water was used in sample preparation. The 1,000 mg/L of stock solution of MB dye was prepared by dissolving an appropriate amount of MB dye in deionized water. Further working solutions were prepared by diluting this stock solution. Initial pH was adjusted using 0.01 N H_2SO_4 and 0.01 N NaOH.

The main instruments used during the study were pH meter (Model 827, Metrohm) equipped with a combined glass-saturated calomel electrode calibrated with buffer solutions of pH 4.0, 7.0, and 9.2, laboratory mesh sieves of 50, 60, 100, and 120, stirrer (Model HP-3000, Lab. Companion), scanning electron microscopy (SEM, JEOL JSM-6380) was used to observe the surface morphology of adsorbent, FTIR spectrophotometer (Model Nicolet 6700, Thermo Scientific, USA), program controller JEIO TECH (Model CF-02G Korea), and UV–vis spectrometer (Model V-530) at a wavelength of 663 nm.

2.2. Adsorbent preparation

Rice agricultural wastes (rice straw) was first washed several times with deionized water to remove dirt, dust, and other impurities, and then dried in the oven at 105˚C for 24 h and then crushed. The rice straw powder was impregnated with concentrated H_2SO_4 in 1:1 ratio then, dried in the oven at 110˚C for 24 h. The sample was carbonized in the furnace at 450˚C with the heating rate at 10˚C/min for 5 h.

During the activation step, the carbonized material was placed in a glass reactor installed in the microwave cavity with the input power and activation time of 700 W and 20 min, respectively. After activation, the activated was washed with distilled water to remove the free acid and the activated carbon was then soaked in KOH solution to remove the remaining acid traces. Then, it was washed with distilled water until the pH of the activated carbon reached 6.5, dried at 105˚C, and sieved to different particle sizes.

2.3. Batch sorption study

Batch experiments were conducted to investigate the effects of influential parameters such as solution pH, adsorbent dose, contact time, initial adsorbate concentration, stirring speed, and temperature on adsorption of the dye from the aqueous solution. All the adsorption experiments were carried out at room temperature (25 ± 2˚C). Adsorption experiments were carried out in 100 mL Erlenmeyer flasks containing amount of carbon prepared and 50 mL of dye solution with known concentration, pH value, and temperature. The agitator stirring speed was 150 rpm. After a preset contact time, the samples were separated from the solution by filtration through the filter paper. The exact concentration of the residual dye in the filtrate was determined using UV–vis spectrometer at a wavelength of maximum absorbance (663 nm). The amount of dye adsorbed on the carbon was calculated from the difference between the initial concentration of dye and the residual dye. The results were expressed as the removal efficiency (%) of the adsorbent toward dye, which was defined as:

$$\text{Removal efficiency } (\%) = \left(\frac{C_0 - C_f}{C_0}\right) \times 100 \quad (1)$$

where C_0 is the initial dye concentrations (mg/L) and C_f is final concentrations (mg/L).

The adsorption capacity of dye is the concentration of dye on the adsorbent mass and was calculated based on the mass balance principle:

$$q_e = \frac{V(C_0 - C_t)}{W} \quad (2)$$

where q_e is the amount of dye adsorbed by the carbon (mg MB/g carbon), C_t is the dye concentration at time t in the solution (mg/L), V is the volume of the dye solution (L), and W is the weight of carbon added into the solution (g).

2.4. Adsorption kinetics

The study of chemical kinetics includes careful monitoring of the experimental conditions which influence the speed of a chemical reaction and helps to attain equilibrium in a reasonable length of time. Various kinetic models, namely pseudo-first-order, pseudo-second-order, intra-particle diffusion, and Elovich model [25–27] have been used for their validity with the experimental adsorption data for MB onto activated carbon prepared from rice agricultural wastes.

2.4.1. Pseudo-first-order kinetic model

Lagergren suggested a pseudo-first-order equation for the sorption of liquid/solid system based on solid capacity [25]. The integral form of pseudo-first-order kinetic model can be expressed as follows:

$$q_t = q_e(1 - e^{-K_1 t}) \quad (3)$$

where q_e and q_t are the amount of MB adsorbed (mg/g) at equilibrium and time t, respectively; and K_1 is the rate constant of pseudo-first-order kinetic model (g/mg min).

2.4.2. Pseudo-second-order model

Ho and Mckay developed a pseudo-second-order equation based on the amount of sorbed sorbate on the sorbent [28]. The pseudo-second-order kinetic model can be presented by the integral equation:

$$q_t = \frac{t}{\frac{1}{K_2 q_e^2} + \frac{t}{q_e}} \quad (4)$$

where q_e and q_t are the amount of MB absorbed (mg/g) at equilibrium and time t, respectively; and K_2 is the rate constant of pseudo-second-order kinetic model (g/mg min).

2.4.3. Intra-particle diffusion model

The adsorption mechanism of a sorbate onto the adsorbent follows three steps viz. film diffusion, pore diffusion, and intra-particle transport. The slowest of the three steps controls the overall rate of the process. Generally, pore diffusion and intra-particle diffusion are often rate-limiting in a batch reactor, which for continuous flow system film diffusion is more likely the rate limiting step. The adsorption rate parameter

which controls the batch process for most of the contact time is the intra-particle diffusion [29,30]. The initial rate of intra-particle diffusion can be calculated by plotting q_t vs. $t^{1/2}$.

$$k_p = \frac{q_t}{t^{\frac{1}{2}}} \tag{5}$$

In which q_t is amount of MB on the surface of the sorbent at time t, (mg/g), k_p is the intra-particle rate constant (mg/g min), t is the time (min).

2.4.4. Elovich equation

The Elovich equation [31] has been used in the following form:

$$q_t = \beta \ln(\alpha\beta) + \beta \ln t \tag{6}$$

It is postulated that the Elovich constants a and b, represent the initial adsorption rate (g/mg min) and the desorption constant (mg/g min), respectively. The Elovich constants could be computed from the plots of q_t vs. ln t.

2.5. Adsorption thermodynamics

The temperature influences the adsorption equilibrium and its variations produce a displacement from or toward the phase the solubility of the molecules (if in liquid phase) and their diffusion within the pores of the adsorbent materials [32]. The free energy change (ΔG°), enthalpy change (ΔH°), and entropy change (ΔS°) were determined by the following equations:

$$\Delta G^\circ = -RT \ln\left(\frac{q_e}{C_e}\right) \tag{7}$$

$$\Delta G^\circ = \Delta H^\circ - T\Delta S^\circ \tag{8}$$

where R is the gas constant (8.314 J/mol L), and T is the absolute temperature (K). The ΔH° and ΔS° can be obtained by plotting ΔG° vs. T.

2.6. Adsorption isotherms

Adsorption isotherms are important in predictive modeling the procedures for designing the adsorption system, because the adsorption capacity of a quantitative of adsorbent could be described, and it helps in making the selection of appropriate adsorbent and determination of adsorbent dosage feasible [33]. Several isotherm models are available. In this study, the adsorption isotherm data were analyzed with Langmuir, Freundlich, Temkin, and Dubinin–Radushkevich isotherms.

2.6.1. Langmuir isotherm model

The Langmuir model assumes that the uptake of adsorbate molecules occurs on a homogenous surface with a finite number of adsorption sites, by monolayer adsorption without any interaction between adsorbed molecules [34]. Once a site is occupied by adsorbate molecules, no further adsorption can occur at that site. The surface will reach the saturation point and the maximum adsorption of the surface will be achieved. To ensure equilibrium conditions, the linear form of the Langmuir isotherm model was applied to the experimental data as [35]:

$$\frac{C_e}{q_e} = \frac{1}{bq_m} - \frac{C_e}{q_m} \tag{9}$$

where C_e, q_m, and K_L are the concentration of adsorbate at equilibrium (mg/L), maximum adsorption capacity (mg/g), and Langmuir constant (L/mg), respectively. The essential characteristics of the Langmuir isotherm can also be expressed in terms of a dimensionless constant separation factor or equilibrium parameter (R_L), which is defined by Eq. (10):

$$R_L = \frac{1}{1 + K_L C_0} \tag{10}$$

where C_0 is the highest initial solute concentration and K_L is the Langmuir's adsorption constant (L/mg). The R_L value confirms the adsorption to be unfavorable ($R_L > 1$), linear ($R_L = 1$), favorable ($0 < R_L < 1$), or irreversible ($R_L = 0$) [36].

2.6.2. Freundlich isotherm model

Freundlich isotherm is the earliest known relationship describing the non-ideal and reversible adsorption; it is not restricted to the formation of monolayer. This empirical model can be applied to multilayer adsorption, with non-uniform distribution of adsorption heat and affinities over the heterogeneous surface [37]. At present, Freundlich isotherm is widely applied in heterogeneous systems especially for organic compounds or highly interactive species on activated carbon and molecular sieves. The empirical Freundlich isotherm is given by Eqs. (11) and (12):

$$q_e = K_F C_e^{\frac{1}{n}} \quad (11)$$

$$\ln q_e = \ln K_F + \frac{1}{n} C_e \quad (12)$$

where q_e is the amount adsorbed (mg/g) and C_e is the equilibrium concentration of the adsorbate (mg/L). The K_F (constant related to adsorption capacity) and $1/n$ (constant related with the adsorption intensity) are Freundlich constants. The value of n is an indication of the favorability of adsorption. Values of $n > 1$ represent favorable nature of adsorption [31].

2.6.3. Temkin isotherm model

The Temkin isotherm model assumes that the adsorption energy decreases linearly with the surface coverage due to adsorbent–adsorbate interactions. The linear form of Temkin isotherm model is described as follows [38]:

$$q_e = \frac{RT}{B_T} \ln K_T + \frac{RT}{B_T} \ln C_e \quad (13)$$

where B_T is the Temkin constant related to the heat of sorption (kJ/mol), K_T is the equilibrium binding constant corresponding to the maximum binding energy (L/g), T is the absolute temperature (K), and R is the gas constant (8.314×10^{-3} kJ/mol K).

2.6.4. Dubinin–Radushkevich isotherm model

Sorption energy was calculated by Dubinin–Radushkevich [39] isotherm model to predict the nature of adsorption process, i.e. physical or chemical. The linear from of the model is described as:

$$\ln q_e = \ln q_m - k_d \varepsilon^2 \quad (14)$$

The Polanyi potential [40] which is equal to:

$$\varepsilon = RT \ln\left(1 + \frac{1}{C_e}\right) \quad (15)$$

where q_e is the amount of MB adsorbed per unit mass of adsorbents, q_m is the theoretical adsorption capacity (mg/g), k_d is a constant related to adsorption energy, and e is Polanyi potential, and can be correlated as:

$$E = \frac{1}{\sqrt{2k_d}} \quad (16)$$

The E (kJ/mol) value gives the information about sorption type, physical or chemical. If $E < 8$ kJ/mol, the adsorption process was physical in nature and in the 8–16 kJ/mol range, and it was chemical in nature [41].

3. Results and discussion

3.1. Characterization of the product

Fig. 1(a) shows the SEM images of raw RS sample. As shown in Fig. 1(a), the surface of untreated RS was homogeneous, smooth, and flat. After activation, the surface was rough and porous in nature (Fig. 1(b)), it is due to the dehydrating action of activating agent, which leads to the porosity development.

Fig. 2(a) and (b) show the FTIR absorption spectra of RS and RSAC. A broad band at around 3,420 cm^{-1} is attributed to hydroxyl (OH) stretching of cellulose and lignin in macro-molecular association. The bands around 2,920 cm^{-1} are assigned to the asymmetric and symmetric stretching, respectively, of the CH_2-group, which constitutes the majority of the aliphatic fractions of the waxes on the rice straw surface [42]. The band in the region of 1,600 (1,622 and 1,624 cm^{-1}) is due to the vibration of aromatic rings present in lignin [43]. The 1,427 cm^{-1} band attributed to lactone structure. The 1,100 cm^{-1} peak corresponds to C–O stretching vibration and O–H bending modes of alcoholic, phenolic, and carboxylic groups [44]. The peak at 1,060 and 1,093 cm^{-1} that is dominant in RS and RSAC samples due to C–O–C type structure [45]. The FTIR spectrum of RSAC (Fig. 2(b)) indicates significant changes after activation. These shifts in peak frequencies indicate that there were binding processes taking place on the surface of carbon. In Fig. 2(c), the changes in peaks intensity show that a binding process was taken place on the surface of the adsorbents after sorption of MB.

3.2. Effect of the solution pH on the adsorption

The initial pH plays an important role in the surface binding sites of the adsorbents and the whole adsorption process. In this work, 50 mL of dye solution of 40 mg/L initial concentration in the pH range of 3–11 was agitated with 0.05 g of RSAC. At lower pH, H^+ may compete with dye ions for the adsorption sites of adsorbent surface, because MB is a cationic dye. Therefore, due to strong repulsive force between dyes and adsorbent, the dye ions uptake was decreased on the surfaces of the adsorbent with the decrease in pH. For higher pH, the competing effect of H^+ ions decreased and the positively charged dye

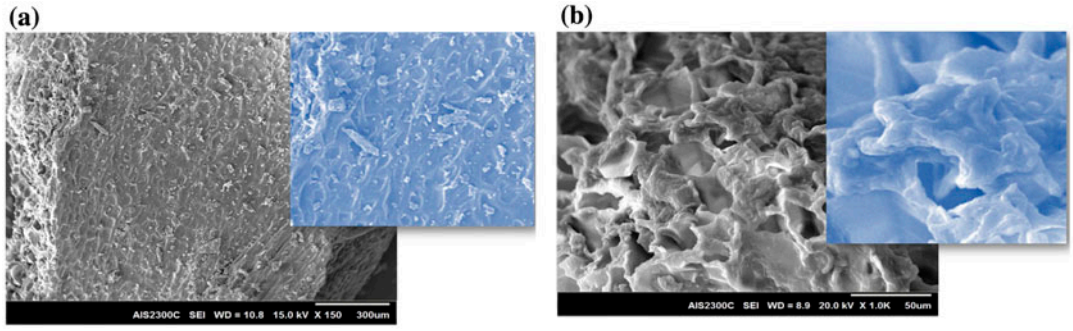

Fig. 1. SEM image of (a) RS and (b) RSAC.

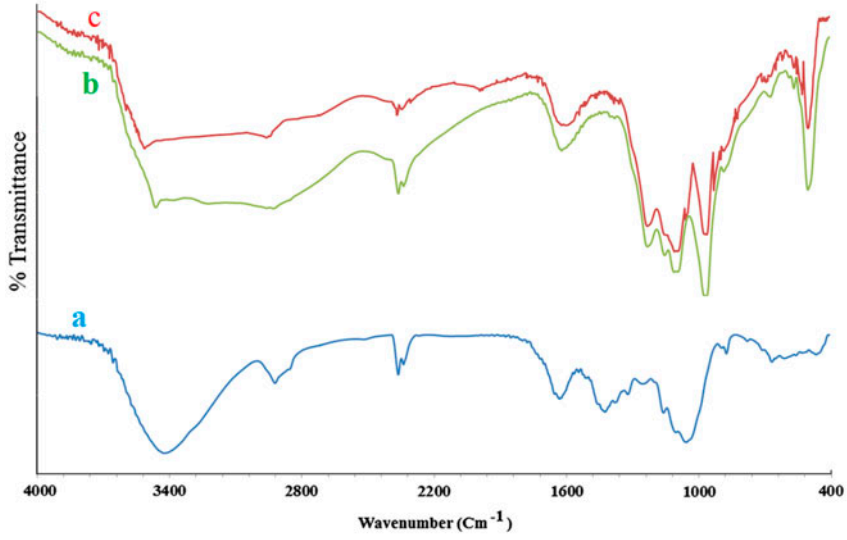

Fig. 2. FTIR spectrum of (a) RS, (b) RSAC, and (c) RSAC after sorption of MB.

ions hook up the free binding sites [46]. According Fig. 3(a), increase dye solution pH from 3 to 11 leads to the improvement in the adsorption removal percentage of MB from 94.37 to 97.5.

The mechanism of MB adsorption by RSAC may be accomplished through both the hydrogen bonding and electrostatic attractions with surface hydroxyl groups which can be given as [47]:

$$AC\text{–}O\text{–}H \rightarrow AC\text{–}O^{-} + H^{+}$$

$$AC\text{–}O^{-} + MB^{+} \rightarrow (ACO)\_MB$$

3.3. Effect of particle size on the adsorption

The effect of adsorbent particle size for an initial MB concentration of 40 mg/L is shown in Fig. 3(b). The experiments were carried out using RSAC with different particle sizes (125–297 μm). The result shows that adsorption increases with an increase in particle size of RSAC. It is obvious that smaller adsorbent particles, which have greater solid–liquid interfacial area, will have the higher adsorption rates. This may be due to an increase in the accessibility of the adsorbate to the pores of the adsorbent with the decrease in adsorbent particle size.

3.4. Effect of adsorbent dosage on the adsorption

Adsorbent dosage also plays an important role in the adsorption process, because it determines the capacity of an adsorbent for a given initial concentration of the adsorbate. Effect of adsorbent dosage was studied using a dose of RSAC from 0.03 to 0.1 g/L that was shown in Fig. 3(c). The effect of adsorbent dosage was studied on dye ion removal, the other parameters were fixed. According to Fig. 3(c), as the

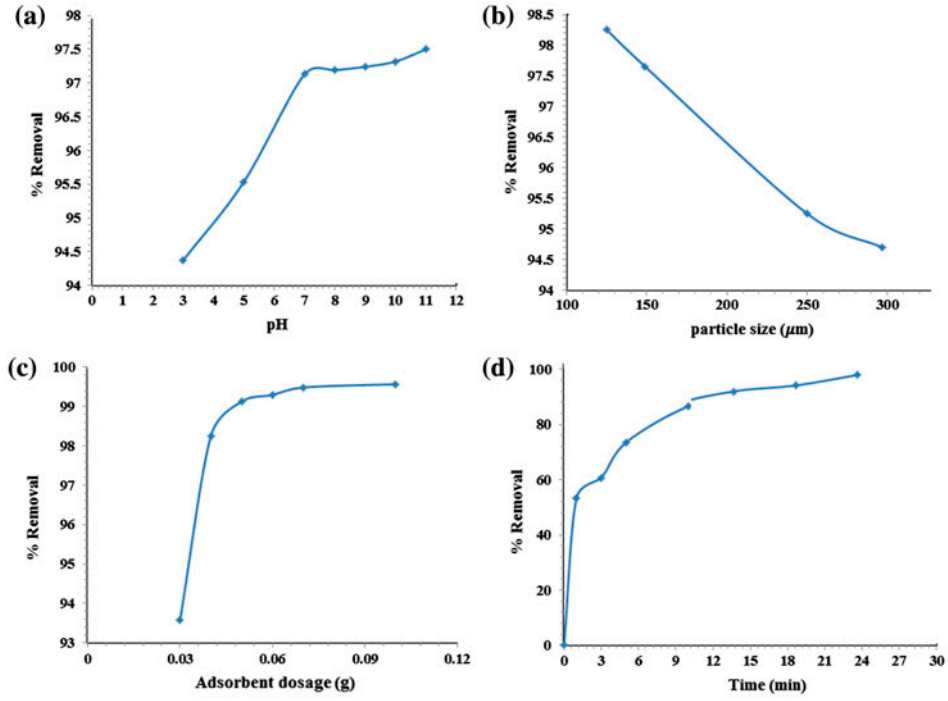

Fig. 3. (a) Effect of pH on the sorption of MB, (b) effect of adsorbent particle size on the sorption of MB, (c) effect of adsorbent dosage on the sorption of MB, and (d) effect of contact time on the sorption of MB.

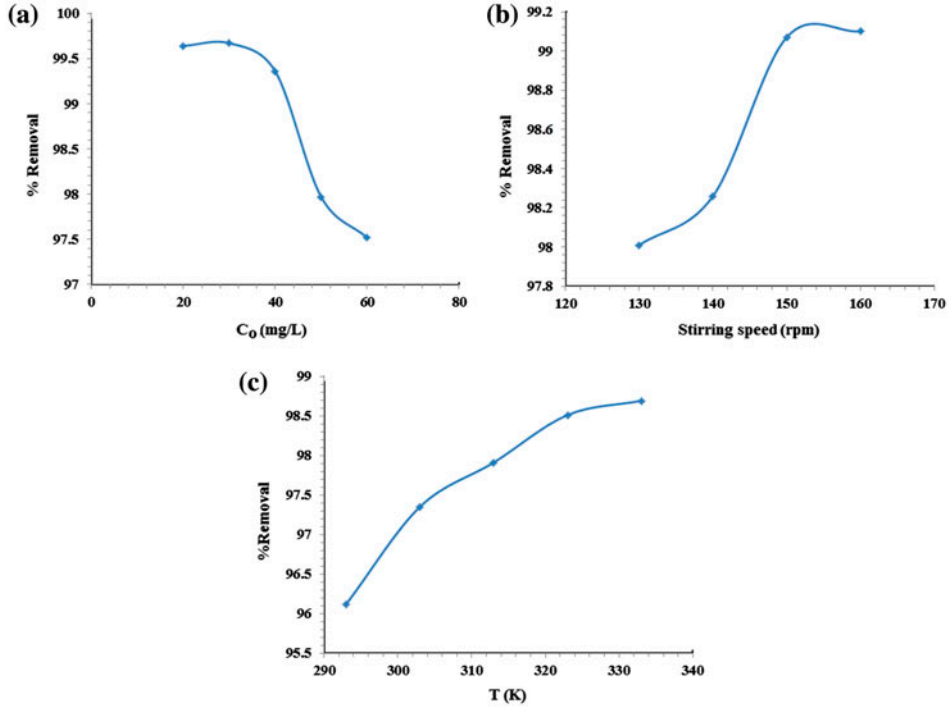

Fig. 4. (a) Effect of initial dye concentration on the sorption of MB, (b) effect of stirring speed on the sorption of MB, and (c) effect of temperature on the sorption of MB.

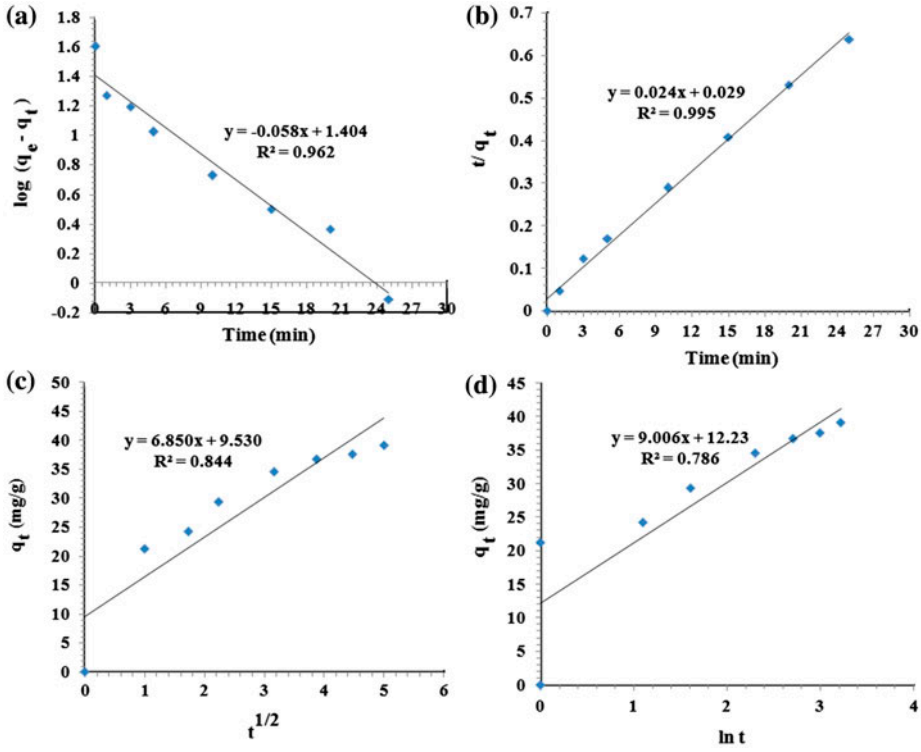

Fig. 5. Adsorption kinetic models for sorption of MB (a) pseudo-first-order, (b) pseudo-second-order, (c) intra-particle diffusion, and (d) Elovich model.

Table 1
The adsorption kinetics of MB

Model	Parameter	Adsorbent (RAC)
Pseudo-first-order	$q_{e(exp)}$ (mg/g)	39.992
	q_e (mg/g)	25.351
	K_1 (min^{-1})	0.128
	R^2	0.962
Pseudo-second-order	$q_{e(exp)}$ (mg/g)	39.992
	q_e (mg/g)	41.667
	K_2 (g/mg min)	0.020
	R^2	0.995
Intra-particle diffusion	K_i (mg/g min)	6.850
	I (mg/g)	9.530
	R^2	0.844
Elovich	α (mg/g min)	1.163
	β (mg/g)	9.006
	R^2	0.786

RSAC concentration increases, percentage adsorption generally increases, but the amount adsorbed per unit mass of the RSAC decreases considerably. The decrease in unit adsorption with increase in the dose

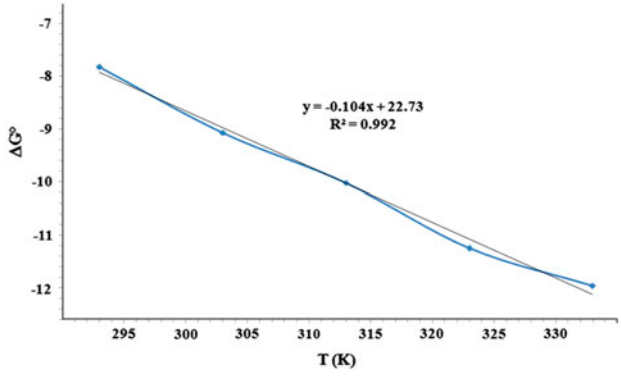

Fig. 6. Changes of ΔG° (kJ/mol) vs. temperature (K).

of RSAC is basically due to adsorption sites remaining unsaturated during the adsorption reaction.

3.5. Effect of contact time on the adsorption

Equilibrium time is one of the most important parameters in the design of economical wastewater treatment systems. These experiments have been carried out at variation of time of contact (0–40 min). After every contact time, one sample was removed

Table 2
Thermodynamic parameters for the adsorption of MB

		ΔG° (kJ/mol)				
ΔH° (kJ/mol)	ΔS° (kJ/mol K)	293 K	303 K	313 K	323 K	333 K
22.73	0.104	−7.819	−9.069	−10.019	−11.252	−11.960

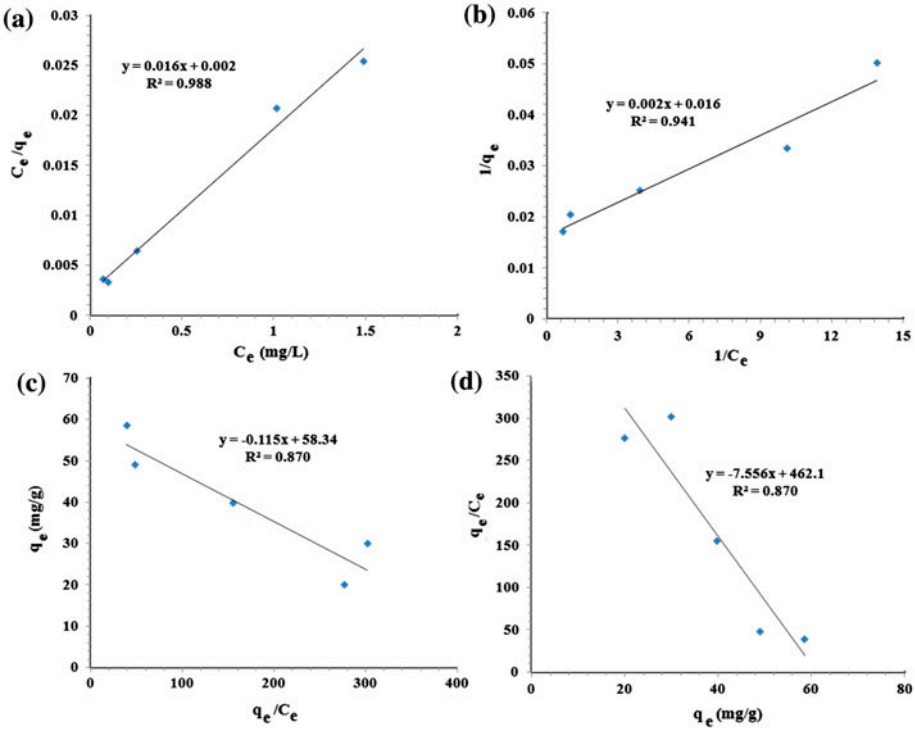

Fig. 7. Langmuir isotherm plots (a) Type 1; (b) Type 2; (c) Type 3; (d) Type 4.

and filtered immediately and the filtrate was analyzed. The result showed that the adsorption of dye ion initially increases with increasing the contact time and then the percentage removal almost constant, i.e. adsorption reaches equilibrium. The time taken to reach the equilibrium was 25 min for RSAC (Fig. 3(d)).

3.6. Effect of initial dye concentration on the adsorption

The effect of initial dye concentration (between 20 and 60 mg/L) on the adsorption of MB onto the RSAC was studied and the results were shown in Fig. 4(a). The adsorption capacity of RSAC increased with increasing initial dye concentration and also percent adsorption decreased with the increase in initial dye concentration. It means that the adsorption is highly dependent on initial concentration of MB. Because at lower dye concentration, the ratio of the initial number of dye molecules to the available adsorbent sites is low and subsequently the fractional adsorption becomes independent of initial dye concentration. However, at high dye concentration the available sites of adsorption becomes fewer and therefore, the percentage removal of MB is dependent upon initial its concentration.

3.7. Effect of stirring speed on the adsorption

Agitation is an important factor in the adsorption phenomena influencing the distribution of the solute in the bulk solution and formation of the external boundary film. The effect of adsorption of MB onto

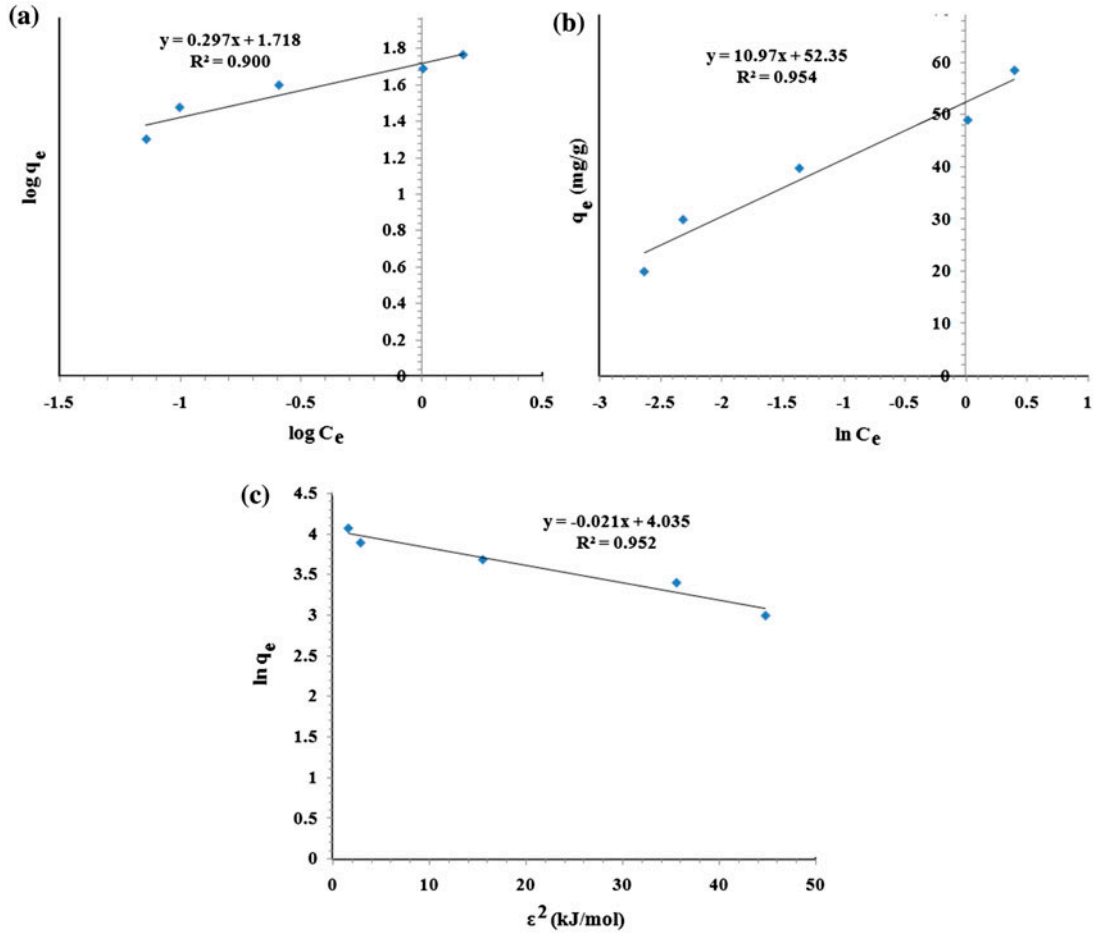

Fig. 8. (a) Freundlich isotherm plot, (b) Temkin isotherm plot, and (c) Dubinin–Radushkevich isotherm plot.

RSAC was studied at different stirring speeds (between 130 and 160 rpm). As shown in Fig. 4(b), the adsorbed dye by RSAC increased with the increase in stirring speed, because all binding sites were available for further adsorption the external mass transfer coefficient increases.

3.8. Effect of temperature on the adsorption

The temperature can affect the adsorption rate. In this study, the effect of temperature on MB adsorption was investigated in the range of 293–333 K. Fig. 4(c) shows the percentage removal of RSAC increased from 96.12 to 98.69, when the temperature was increased from 293 to 333 K. The maximum MB adsorption capacity observed at 333 K was 39.47 mg/g for RSAC. These results are attributed to the increased mobility of MB ions with increasing temperature. With increasing reaction temperature in solution, the amount of nonprotonated functional groups on the adsorbent increases due to the increase in the dissociation constant of the protonated hydroxyl groups. Increasing the temperature is known to increase the rate of diffusion of the adsorbate molecules across the external boundary layer and in the internal pores of the adsorbent particle, owing to the decrease in the viscosity of the dye solution. In addition, changing temperature will change the equilibrium capacity of the adsorbent for a particular adsorbate [48].

3.9. Adsorption kinetic study

In order to investigate the adsorption behavior of MB on RSAC, four kinetic models such as pseudo-first-order, pseudo-second-order, intra-particle diffusion, and Elovich model were used. As seen from Fig. 5, the pseudo-second-order model was found to be more suitable since the values of regression coefficients (R^2) could be regarded as a measure of the appropriate fit of experimental data on the kinetic

Table 3
The adsorption isotherms of MB

Model	Parameter	Adsorbent (RAC)
Langmuir		
Type 1	b (L/mg)	8
	q_m (mg/g)	62.5
	R^2	0.988
Type 2	b (L/mg)	8
	q_m (mg/g)	62.5
	R^2	0.941
Type 3	b (L/mg)	8.696
	q_m (mg/g)	58.34
	R^2	0.870
Type 4	b (L/mg)	7.556
	q_m (mg/g)	61.157
	R^2	0.870
Freundlich	K_F	52.240
	$1/n$	0.297
	n	3.367
	R^2	0.900
Temkin	A_T	118.155
	B_T	10.97
	R^2	0.954
Dubinin–Radushkevich	K_{DR}	0.021
	q_{max}	56.543
	E	4.878
	R^2	0.952

models. The corresponding parameters calculated according to the models and values of regression coefficients were tabulated in Table 1. The measured kinetic data of MB adsorbed by RSAC fitted the pseudo-second-order model with a correlation coefficient of 0.995. This means that the adsorption processes were controlled by the chemical process [49].

3.10. Adsorption thermodynamic study

The investigation of temperature which was expected to have a significant influence on MB adsorption onto RSAC was carried out at the range of 293–333 K. Under different temperatures, the adsorption capacities of the RSAC for MB were measured individually at pH 7.0 with 0.05 g of RSAC and 40 mg/L of initial MB concentration.

The changes of ΔG° (kJ/mol) vs. temperature (K) are shown in Fig. 6. The values of ΔG° increase by increasing of temperature that shows the feasibility of adsorption of MB adsorption onto RSAC. The values of ΔS° (kJ/mol K) and ΔH° (kJ/mol) calculated from Eq. (8) are given as 0.104 kJ/mol K and 22.73 kJ/mol, respectively. All thermodynamic parameters were tabulated in Table 2. The negative values of ΔG° and the positive value of ΔH° indicated that the process was a spontaneous adsorption process and endothermic [50]. The ΔH° positive value might be caused by the removal of water molecules from the solid–solution interface and from the hydrated dye ions [51]. It also indicates that the adsorption of MB onto RSAC is physical adsorption with no chemical bond formation. The positive ΔS° value for MB adsorption on RAC is due to increasing randomness at the solid–solution interface during the adsorption process [52].

3.11. Adsorption isotherm study

The adsorption isotherm of RSAC for MB was investigated at 298 K and the data were analyzed by Langmuir (four types), Freundlich, Temkin, and Dubinin–Radushkevich equations, respectively.

The linear fitting of the adsorption isotherms is shown in Figs. 7 and 8. The fitting constants and regression coefficients (R^2) are tabulated in Table 3. As can be seen from this Table, adsorption of MB by RSAC can be made fit using Type 1, Type 2, Type 3, and Type 4 Langmuir equations. Also, Type 1 equation offers a best correlation factor ($R^2 = 0.988$). The R^2 values indicate that the Langmuir isotherm model was well fitted and in good agreement with the experimental data better than that of the other models at this temperature. Therefore, the adsorptions of MB onto RSAC were monolayer uniform adsorptions [45]. The results of MB adsorption onto various adsorbents from different researchers were shown in Table 4 [53–67]. The differences of MB uptake onto various adsorbents were due to the properties (function groups, particle size, surface area, etc.) of them.

3.12. Desorption of MB from the sorbent

Desorption studies were carried out by batch process. After the adsorption process is done, for desorption experiments, 0.1 M H_2SO_4has been used. In order to show the reusability of the RSAC, adsorption–desorption cycle of MB dye was repeated five times using the same instruction. At first, 50 mL of 40 mg/L MB dye solution was stirred with 0.06 g of RSAC at 25°C for 1 h. After 1 h, the RSAC was washed several times with deionized water to remove excess of dye. Then, RSAC was treated with 50 mL of 0.1 M H_2SO_4 solution in another flask. The flask was again stirred at 25°C in order to desorb MB for 1 h. The solution was then filtered with Whatman filter paper number 42 and the

Table 4
Comparison of the maximum monolayer adsorption of MB onto various adsorbents

Adsorbent	q_m (mg/g)	Refs.
Pineapple stem	119	[53]
Tea waste	85	[54]
Caulerpa racemosa varcylindracea	3.42	[55]
Yellow passion fruit waste	44.7	[56]
Sulfuric acid treated Parthenium	39	[57]
Phosphoric acid treated Parthenium	88	[57]
Pumpkin seed hull	141	[58]
Coir pith carbon	05.87	[59]
Neem (*Azadirachta indica*) leaf powder	19.6	[60]
Neem leaf powder	8.76	[60]
Petrified sediment	2.04	[61]
Glass wool	02.25	[62]
Fly ash	02.63	[63]
Date stones	40	[64]
Palm-trees waste	35	[64]
Posidonia oceanica L. fibers	05.56	[65]
Garlic peel	82.6	[66]
Raw beech sawdust	09.78	[67]
Rice straw activated carbon	62.5	This study

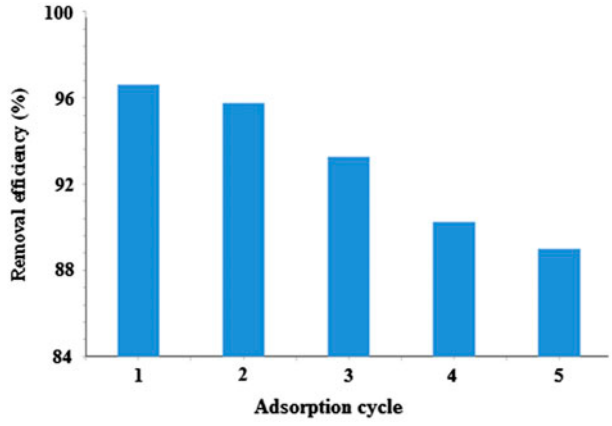

Fig. 9. Adsorption of MB in five cycles.

filtrate was analyzed for MB dye desorbed by RSAC. As shown in Fig. 9, desorption was 93.25% up to the third regeneration cycle. However, desorption decreased up to 88.98% in the fifth cycle.

4. Conclusion

Activated carbon prepared from rice could be used as an effective adsorbent for the efficient removal of MB from aqueous solution. The equilibrium time for rapid adsorption of MB from aqueous solutions was reached within 25 min of contact time and the kinetics data showed better applicability for pseudo-second-order model. The isotherm study indicated that adsorption data were best described by the Langmuir isotherm model as is evident from the high R^2 value of 0.988. The maximum monolayer adsorption capacities for the removal of MB using RSAC adsorbent was found 62.5 mg/g at an initial pH of 7 and a temperature of 298 K. The negative value of ΔG° and the positive values of ΔH° (22.73 kJ/mol) and ΔS° (0.104 kJ/mol K) show that the adsorption process is a spontaneous physical adsorption process, which is endothermic and entropy driven. The results indicate that RSAC adsorbent could be employed as an effective and promising adsorbent for the removal of MB from aqueous solutions.

References

[1] W.A. Al-Amrani, P.-E. Lim, C.-E. Seng, W.S. Wan Ngah, Bioregeneration of azo dyes-loaded monoamine modified silica in batch system: Effects of particle size and biomass acclimation condition, Chem. Eng. J. 251 (2014) 175–182.
[2] S. Mondal, Methods of dye removal from dye house effluent—An overview, Environ. Eng. Sci. 25 (2008) 383–396.
[3] M. Ghaedi, S. Heidarpour, S. Nasiri Kokhdan, R. Sahraie, A. Daneshfar, B. Brazesh, Comparison of silver and palladium nanoparticles loaded on activated carbon for efficient removal of methylene blue: Kinetic and isotherm study of removal process, Powder Technol. 228 (2012) 18–25.

[4] K. Mahapatra, D.S. Ramteke, L.J. Paliwal, Production of activated carbon from sludge of food processing industry under controlled pyrolysis and its application for methylene blue removal, J. Anal. Appl. Pyrol. 95 (2012) 79–86.
[5] J.Z. Yi, L.M. Zhang, Removal of methylene blue dye from aqueous solution by adsorption onto sodium humate/polyacrylamide/clay hybrid hydrogels, Bioresour. Technol. 99 (2008) 2182–2186.
[6] A. Dąbrowski, Adsorption—From theory to practice, Adv. Colloid Interface Sci. 93 (2001) 135–224.
[7] A.E. Ofomaja, Kinetic study and sorption mechanism of methylene blue and methyl violet onto mansonia (*Mansonia altissima*) wood sawdust, Chem. Eng. J. 143 (2008) 85–95.
[8] V.K. Garg, R. Gupta, A. Bala Yadav, R. Kumar, Dye removal from aqueous solution by adsorption on treated sawdust, Bioresour. Technol. 89 (2003) 121–124.
[9] A.R. Tehrani-Bagha, H. Nikkar, N.M. Mahmoodi, M. Markazi, F.M. Menger, The sorption of cationic dyes onto kaolin: Kinetic, isotherm and thermodynamic studies, Desalination 266 (2011) 274–280.
[10] M. Soylak, L. Elci, M. Dogan, Determination of some trace metal impurities in refined and unrefined salts after preconcentration onto activated carbon, Fresenius Environ. Bull. 5 (1996) 148–155.
[11] A. Gundogdu, C. Duran, H.B. Senturk, M. Soylak, D. Ozdes, H. Serencam, M. Imamoglu, Adsorption of phenol from aqueous solution on a low-Cost activated carbon produced from tea Industry waste: Equilibrium, kinetic, and thermodynamic study, J. Chem. Eng. Data 57 (2012) 2733–2743.
[12] M. Soylak, L. Elci, M. Dogan, Uses of activated carbon columns for solid phase extraction studies prior to determinations of traces heavy metal ions by flame atomic absorption spectrometry, Asian J. Chem. 15 (2003) 1735–1738.
[13] T. Robinson, B. Chandran, P. Nigam, Removal of dyes from an artificial textile dye effluent by two agricultural waste residues, corncob and barley husk, Environ. Int. 28 (2002) 29–33.
[14] H. Aydın, G. Baysal, Adsorption of acid dyes in aqueous solutions by shells of bittim (Pistacia khinjuk stocks), Desalination 196 (2006) 248–259.
[15] M. Olivares-Marín, C. Ferna´ndez-Gonza´ lez, A. Macı´as-Garcı´a, V. Go´ mez-Serrano, Preparation of activated carbon from cherry stones by physical activation in air. Influence of the chemical carbonisation with H_2SO_4, J. Anal. Appl. Pyrol. 94 (2012) 131–137.
[16] A.M.M. Vargas, C.A. Garcia, E.M. Reis, E. Lenzi, W.F. Costa, V.C. Almeida, NaOH-activated carbon from flamboyant (*Delonix regia*) pods: Optimization of preparation conditions using central composite rotatable design, Chem. Eng. J. 162 (2010) 43–50.
[17] W. Liu, J. Zhang, C. Zhang, Y. Wang, Y. Li, Adsorptive removal of Cr(VI) by Fe-modified activated carbon prepared from *Trapa natans* husk, Chem. Eng. J. 162 (2010) 677–684.
[18] A.M.M. Vargas, A.L. Cazetta, C.A. Garcia, J.C.G. Moraes, E.M. Nogami, E. Lenzi, W.F. Costa, V.C. Almeida, Preparation and characterization of activated carbon from a new raw lignocellulosic material: Flamboyant (*Delonix regia*) pods, J. Environ. Manage. 92 (2011) 178–184.
[19] K. Yang, J. Peng, H. Xia, L. Zhang, C. Srinivasakannan, S. Guo, Textural characteristics of activated carbon by single step CO_2 activation from coconut shells, J. Taiwan Inst. Chem. Eng. 41 (2010) 367–372.
[20] J. Yang, K. Qiu, Preparation of activated carbons from walnut shells via vacuum chemical activation and their application for methylene blue removal, Chem. Eng. J. 165 (2010) 209–217.
[21] M. Auta, B.H. Hameed, Optimized waste tea activated carbon for adsorption of methylene blue and acid blue 29 dyes using response surface methodology, Chem. Eng. J. 175 (2011) 233–243.
[22] M. Ghasemi, M.Z. Khosroshahy, A.B. Abbasabadi, N. Ghasemi, H. Javadian, M. Fattahi, Microwave-assisted functionalization of *Rosa canina*-L fruits activated carbon with tetraethylenepentamine and its adsorption behavior toward Ni(II) in aqueous solution: Kinetic, equilibrium and thermodynamic studies, Powder Technol. 274 (2015) 362–371.
[23] S. Kumagai, M. Sato, D. Tashima, Electrical double-layer capacitance of micro- and mesoporous activated carbon prepared from rice husk and beet sugar, Electrochim. Acta 114 (2013) 617–626.
[24] K.Y. Foo, B.H. Hameed, Utilization of rice husks as a feedstock for preparation of activated carbon by microwave induced KOH and K_2CO_3 activation, Bioresour. Technol. 102 (2011) 9814–9817.
[25] S. Lagergren, Zur theorie der sogenannten adsorption gel¨oster stoffe (About the theory of so-called adsorption of soluble substances), Kungliga Svenska Vetenskapsakademiens, Handlin. 24 (1898) 1–39 (in German).
[26] Y.S. Ho, G. McKay, Sorption of dye from aqueous solution by peat, Chem. Eng. J. 70 (1998) 115–124.
[27] W.J. Weber, J.C. Morris, Kinetics of adsorption on carbon from solution, J. Sanit. Eng. Div. 89 (1963) 31–59.
[28] Y.S. Ho, Review of second-order models for adsorption systems, J. Hazard. Mater. 136 (2006) 681–689.
[29] S. Coswami, U.C. Ghosh, Studies on adsorption behaviour of Cr(VI) onto synthetic hydrous stannic oxide, Water SA 31 (2005) 597–602.
[30] H. Javadian, Application of kinetic, isotherm and thermodynamic models for the adsorption of Co(II) ions on polyaniline/polypyrrole copolymer nanofibers from aqueous solution, J. Ind. Eng. Chem. 20 (2014) 4233–4241.
[31] P.K. Malik, Dye removal from wastewater using activated carbon developed from sawdust: Adsorption equilibrium and kinetics, J. Hazard. Mater. 113 (2004) 81–88.
[32] L.M. Cotoruelo, M.D. Marqués, F.J. Díaz, J.R. Mirasol, J.J. Rodríguez, T. Cordero, Adsorbent ability of lignin-based activated carbons for the removal of p-nitrophenol from aqueous solutions, Chem. Eng. J. 184 (2012) 176–183.
[33] U. Kumar, M. Bandyopadhyay, Sorption of cadmium from aqueous solution using pretreated rice husk, Bioresour. Technol. 97 (2006) 104–109.
[34] H. Deng, L. Yang, G. Tao, J. Dai, Preparation and characterization of activated carbon from cotton stalk by microwave assisted chemical activation—Application in methylene blue adsorption from aqueous solution, J. Hazard. Mater. 166 (2009) 1514–1521.

[35] H. Javadian, M. Taghavi, Application of novel polypyrrole/thiol-functionalized zeolite Beta/MCM-41 type mesoporous silica nanocomposite for adsorption of Hg^{2+} from aqueous solution and industrial wastewater: Kinetic, isotherm and thermodynamic studies, Appl. Surf. Sci. 289 (2014) 487–494.
[36] S.M. Nasehi, S. Ansari, M. Sarshar, Removal of dark colored compounds from date syrup using activated carbon: A kinetic study, J. Food Eng. 111 (2012) 490–495.
[37] K.Y. Foo, B.H. Hameed, Insights into the modeling of adsorption isotherm systems, Chem. Eng. J. 156 (2010) 2–10.
[38] B. Kiran, A. Kaushik, Chromium binding capacity of *Lyngbya putealis* exopolysaccharides, Biochem. Eng. J. 38 (2008) 47–54.
[39] H. Javadian, P. Vahedian, M. Toosi, Adsorption characteristics of Ni(II) from aqueous solution and industrial wastewater onto Polyaniline/HMS nanocomposite powder, Appl. Surf. Sci. 284 (2013) 13–22.
[40] H. Javadian, M. Angaji, M. Naushad, Synthesis and characterization of polyaniline/γ-alumina nanocomposite: A comparative study for the adsorption of three different anionic dyes, J. Ind. Eng. Chem. 20 (2014) 3890–3900.
[41] T.K. Naiya, A.K. Bhattacharya, S.N. Mandal, S.K. Das, The sorption of lead(II) ions on rice husk ash, J. Hazard. Mater. 163 (2009) 1254–1264.
[42] Zh Liu, X. Zhou, X. Chen, Ch Dai, J. Zhang, Y. Zhang, Biosorption of clofibric acid and carbamazepine in aqueous solution by agricultural waste rice straw, J. Environ. Sci. 25 (2013) 2384–2395.
[43] I. Kim, M. Saif Ur Rehman, J.-I. Han, Fermentable sugar recovery and adsorption potential of enzymatically hydrolyzed rice straw, J. Cleaner Prod. 66 (2014) 555–561.
[44] S.M. Yakout, S.S. Metwally, T. El-Zakla, Uranium sorption onto activated carbon prepared from rice straw: Competition with humic acids, Appl. Surf. Sci. 280 (2013) 745–750.
[45] G.H. Oh, C.R. Park, Preparation and characteristics of rice-straw-based porous carbons with high adsorption capacity, Fuel 81 (2002) 327–336.
[46] G. Zhang, Y. Bao, Study of adsorption characteristics of methylene blue onto activated carbon made by salix psammophila, Energy Proc. 16 (2011) 1141–1146.
[47] G.R. Bardajee, Z. Hooshyar, F.E. Shahidi, Synthesis and characterization of a novel Schiff-base/SBA-15 nanoadsorbent for removal of methylene blue from aqueous solutions, Int. J. Environ. Sci. Technol. 12 (2015) 1737–1748.
[48] Z. Al-Qodah, Adsorption of dyes using shale oil ash, Water Res. 34 (2000) 4295–4303.
[49] X. Xin, Q. Wei, J. Yang, L. Yan, R. Feng, G. Chen, B. Du, H. Li, Highly efficient removal of heavy metal ions by amine-functionalized mesoporous Fe_3O_4 nanoparticles, Chem. Eng. J. 184 (2012) 132–140.
[50] Y.H. Li, Z. Di, J. Ding, D. Wu, Z. Luan, Y. Zhu, Adsorption thermodynamic, kinetic and desorption studies of Pb^{2+} on carbon nanotubes, Water Res. 39 (2005) 605–609.
[51] P. Miretzky, C. Muñoz, E. Cantoral-Uriza, Cd^{2+} adsorption on alkaline pretreated diatomaceous earth: Equilibrium and thermodynamic studies, Environ. Chem. Lett. 9 (2011) 55–63.
[52] Q. Li, L. Chai, W. Qin, Cadmium(II) adsorption on esterified spent grain: Equilibrium modeling and possible mechanisms, Chem. Eng. J. 197 (2012) 173–180.
[53] B.H. Hameed, A.A. Ahmad, Batch adsorption of methylene blue from aqueous solution by garlic peel, an agricultural waste biomass, J. Hazard. Mater. 164 (2009) 870–875.
[54] Md.T. Uddin, Md.A. Islam, S. Mahmud, Md. Rukanuzzaman, Adsorptive removal of methylene blue by tea waste, J. Hazard. Mater. 164 (2009) 53–60.
[55] S. Cengiz, L. Cavas, Removal of methylene blue by invasive marine sea weed: *Caulerpa racemosavar* cylindracea, Bioresour. Technol. 99 (2008) 2938–2946.
[56] F.A. Pavan, E.C. Lima, S.L.P. Dias, A.C. Mazzocato, Methylene blue biosorption from aqueous solutions by yellow passion fruit waste, J. Hazard. Mater. 150 (2008) 703–712.
[57] H. Lata, V.K. Garg, R.K. Gupta, Removal of a basic dye from aqueous solution by adsorption using *Parthenium hysterophorus*: An agricultural waste, Dyes Pigm. 74 (2007) 653–658.
[58] B.H. Hameed, M.I. El-Khaiary, Removal of basic dye from aqueous medium using a novel agricultural waste material: Pumpkin seed hull, J. Hazard. Mater. 155 (2008) 601–609.
[59] D. Kavitha, C. Namasivayam, Experimental and kinetic studies on methylene blue adsorption by coir pith carbon, Bioresour. Technol. 98 (2007) 14–21.
[60] K.G. Bhattacharyya, A. Sharma, Kinetics and thermodynamics of methylene blue adsorption on Neem (*Azadirachta indica*) leaf powder, Dyes Pigm. 65 (2005) 51–59.
[61] A.Z. Aroguz, J. Gulen, R.H. Evers, Adsorption of methylene blue from aqueous solution on pyrolyzed petrified sediment, Bioresour. Technol. 99 (2008) 1503–1508.
[62] S. Chakrabarti, B.K. Dutta, On the adsorption and diffusion of Methylene Blue in glass fibers, J. Colloid Interface Sci. 286 (2005) 807–811.
[63] V.V.B. Rao, S.R.M. Rao, Adsorption studies on treatment of textile dyeing industrial effluent by fly ash, Chem. Eng. J. 116 (2006) 77–84.
[64] Z. Belala, M. Jeguirim, M. Belhachemi, F. Addoun, G. Trouvé, Biosorption of basic dye from aqueous solutions by date stones and palm-trees waste: Kinetic, equilibrium and thermodynamic studies, Desalination 271 (2011) 80–87.
[65] M.C. Cibi, B. Mahjoub, M. Seffen, Kinetic and equilibrium studies of methylene blue biosorption by *Posidonia oceanica* (L.) fibres, J. Hazard. Mater. 139 (2007) 280–285.
[66] B.H. Hameed, Grass waste: A novel sorbent for the removal of basic dye from aqueous solution, J. Hazard. Mater. 166 (2009) 233–238.
[67] F.A. Batzias, D.K. Sidiras, Dye adsorption by calcium chloride treated beech sawdust in batch and fixed bed systems, J. Hazard. Mater. 114 (2004) 167–174.